CRYO/97/001
October 15, 1997

AC loss calculation algorithm

L. Bottura, C. Rosso

Distribution: C. Marinucci (EPFL-CRPP), C. Luongo, B. Parsons (Bechtel), M. Shimada (Toshiba), N. Mitchell, H. Takigami (ITER JWS), R. Heller (FzK)

Summary

We describe the calculation algorithm for AC loss calculation in superconducting cables presently implemented in M'C, version 2.5. The algorithm takes into account two loss components, hysteresis and coupling. Field penetration and screening are well approximated, allowing to deal with small and fast field cycles (minor loops).

1. Introduction

A superconducting cable subjected to changes of the magnetic field or of the operating current will dissipate power, the so called AC loss. This power must be calculated accurately in order to estimate the cooling power needed to maintain the magnet at the operating temperature. Here we will show how the main AC loss components can be computed with sufficient accuracy using simple analytical models. The AC loss can be split into two main origins:

- hysteresis loss in the superconducting filaments;
- coupling loss within strands and among strands in a cable or composite.

The first component, hysteresis loss, is caused by persistent currents induced in the filament by field changes. These currents shield the filament interiors and produce a magnetization of hysteretic nature. Hysteresis loss involves thus the superconducting filaments only. The second component, coupling loss, is originated by electromagnetic coupling among filaments in a strand, and among strands in a cable. Hence these coupling currents flow partially in the superconductor, partially in resistive contacts among them, and they dissipate power in the resistive transition. Coupling losses thus involve the cable as a whole unit. The next sections deal with each component separately in detail, proposing a flexible calculation algorithm to cope with most practical situations in a superconducting magnet.

2. Hysteresis loss

The calculation of hysteresis loss in a superconducting filament can be quite a complex task, especially when the magnetic field variation is arbitrary. Here an approximate approach is followed, based on the following assumptions:

- the change of each magnetic field component is treated independently, that is the effect of variation of each component is independent from the variation of the other two components. The only coupling between field components arises through the value of the critical current density;
- the critical current is assumed to be uniform throughout the filament cross section;
- transport current effects are neglected.

Undere these assumptions the magnetic and electric field profiles inside the filament could be computed. In practice this is possible for a cylindrical filament in parallel field, but remains a complex task for a cylindrical filament in transverse field. Therefore, in addition to the assumptions above, we approximate a cylindrical filament in a transverse field with a slab of appropriate scaled thickness (see later for the scaling). We are now ready to proceed in the solution of the two cases needed, namely the slab and the cylinder in a *parallel* varying field.

2.1 Slab in parallel field

We start introducing the following normalisation quantities:

- critical current density at zero field $J_{c0}=J_c(0)$
- virgin penetration field $H_{p0}=J_{c0}\,D_{eff}/2$

where D_{eff} is the scaled effective filament diameter (see later), and we normalise all variables as follows:

- space co-ordinate $x = X / D_{eff}/2$
- critical current density $j = J_c(B) / J_{c0}$
- magnetic field $h = H / H_{p0}$
- magnetization $m = M / H_{p0}$
- electric field $e = E / m_0 H_{p0} D_{eff}/2$
- power $p = P / m_0 H_{p0}^2$

Using the normalised quantities, the equations governing the field penetration in a superconducting slab can be written as follows (indexes of components are not

indicated as all vectors have a single component, namely z for the magnetic field and y for the current density and eletric field):

$$\frac{\partial h}{\partial x} = \pm j \tag{2.1}$$

$$\frac{\partial e}{\partial x} = \frac{\partial h}{\partial t} \tag{2.2}.$$

The sign of the current density on r.h.s. in Eq. (2.1) is determined by the direction of the field change and the previous history. The solution of Eq. (2.1) for the penetration layer can be readily found under the assumption of constant j inside the slab (equal - in the Bean approximation - to the critical current value corresponding to the applied external field):

$$h = \begin{cases} h_e + j(1-x) & for \dfrac{\partial h}{\partial t} < 0 \\ h_e - j(1-x) & for \dfrac{\partial h}{\partial t} > 0 \end{cases} \tag{2.3}$$

where h_e is the normalised external field. Equation (2.3) represents a linear decrease in field inside the slab, as shown in Fig. 1. Note that two cases must be considered for the progress of the penetration layer inside the slab, namely the case of penetration of a virgin slab (no previous shielding current layer) and the case of the penetration of a previously established shielding layer. The field profile has the same slope, starting from the external value h_e at x=1, but the penetration depth x_p is different in the two cases. In fact, x_p is given by:

$$x_p = \begin{cases} 1 - \dfrac{|h_e|}{j} & virgin \\ 1 - \dfrac{|h_e|}{2j} & nonvirgin \end{cases} \tag{2.4}.$$

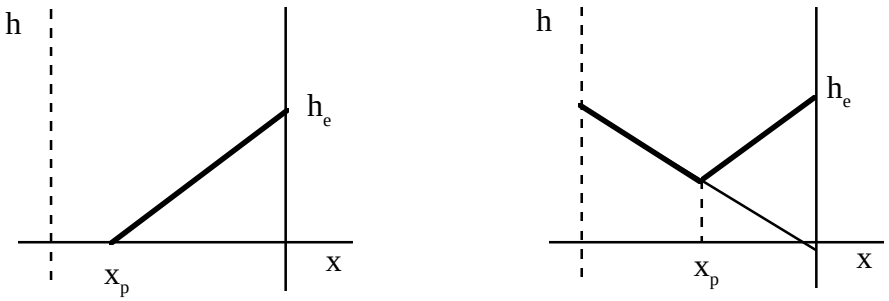

Figure 1. Penetration of the magnetic field in a superconducting slab. Case of virgin slab (left) and previously penetrated slab (right).

The electric field in the penetration layer (between x_p and 1) is given by:

$$e = \dot{h}_e \left(x - x_p \right) \tag{2.5}$$

and is zero outside the penetration layer. The local value of the dissipated power density is obtained as the product of the electric field and current density in the penetration layer:

$$p = \dot{h}_e \, j \left(x - x_p \right) \tag{2.6}.$$

From Eq. (2.6) we can compute the average power density in the slab:

$$\begin{aligned} \overline{p} &= \int_{x_p}^{1} \dot{h}_e \, j \left(x - x_p \right) dx \\ &= \dot{h}_e \, j \, \frac{\left(1 - x_p \right)^2}{2} \end{aligned} \tag{2.7}.$$

The final quantity of interest is the average volume magnetization:

$$\overline{m} = \int_{0}^{1} h dx - h_e \tag{2.8}.$$

To obtain it we need to integrate the contribution from all shielding layers in the slab, where the integral of a single layer extending from $x_p^{\,n}$ to $x_p^{\,n+1}$ equals:

$$\int_{x_p^n}^{x_p^{n+1}} h dx = \left(x_p^{n+1} - x_p^n \right) \frac{h\left(x_p^n \right) + h\left(x_p^{n+1} \right)}{2} \tag{2.9}.$$

The general case of arbitrary variation of the magnetic field can be solved keeping track of the shielding layers and their appearance/disappearance as the external field changes. The magnetic field changes are subdivided in swings at constant ramp-rate. The information to be stored consists therefore in the penetration depth x_p of a shielding current layer, the magnetic field h_e that caused it and the direction of the shielding currents. This allows the reconstruction of the complete h profile inside the slab (needed to compute the magnetization). Once the normalised power is computed, the energy is obtained by numerical integration in time. Note that it is advantageous to work in scaled coordinates throughout this process. The normalised variables obtained are rescaled at the end of each field swing using the normalization factors given at the beginning of this section.

2.2 Scaling of the slab solution

The solution presented in the previous section for a slab can be scaled to represent the penetration of a cylinder in transverse field. To obtain a good approximation the scaling is done so that the asymptotic behaviour of the equivalent slab and cylinder is the same for small and large field changes. To obtain the scaling, we write the following known expressions for the volume loss energy per cycle Q in the case of a slab in a parallel alternating field with total field swing B_m (peak to peak amplitude of the field change):

$$Q_s = \begin{cases} \dfrac{B_m^2}{2\mu_0}\dfrac{\beta}{3} & for\ \beta \le 1 \\ \dfrac{B_m^2}{2\mu_0}\left(\dfrac{1}{\beta} - \dfrac{2}{3\beta^2}\right) & for\ \beta > 1 \end{cases} \tag{2.10}$$

and in the case of a cylinder in a tranverse alternating field:

$$Q_c = \begin{cases} \dfrac{B_m^2}{2\mu_0}\dfrac{2}{3}\left(2\beta - \beta^2\right) & for\ \beta \le 1 \\ \dfrac{B_m^2}{2\mu_0}\dfrac{2}{3}\left(\dfrac{2}{\beta} - \dfrac{1}{\beta^2}\right) & for\ \beta > 1 \end{cases} \tag{2.11}$$

The parameter β in the two equations above is proportional to the ratio of the field swing to the penetration field B_p:

$$\beta = \frac{B_m}{2B_p} \tag{2.12}$$

where we need finally to remember that the (first) penetrastion field for a slab and a cylinder are given by:

slab: $$B_p = \mu_0 J_c \frac{D_s}{2} \tag{2.13}$$

cylinder: $$B_p = \mu_0 J_c \frac{D_c}{\pi} \tag{2.14}$$

with D_s and D_c respectively slab thickness and cylinder diameter. If we now look at the asymptotic behaviours of slab and cylinder in the limits $\beta \to 0$, and $\beta \to \infty$,

it can be easily verified that we can obtain the same dissipated energy per cycle if we:

- use a slab effective thickness obtained from the effective filament diameter as:
$$D_{eff}^{slab} = \frac{8}{3\pi F} D_{eff}^{cyl} \quad (2.15),$$
- and scale the energy per cycle by the factor F=2.309.

The scaling that we propose is thus based on the use of the analytical slab solution, using the effective slab thickness given by Eq. (2.15) and multiplying the magnetization, power and energy of the equivalent slab by a factor F.

2.3 Cylinder in parallel field

A cylinder in parallel field is described by equations that are very similar to those of a slab, treated previously. Therefore it is possible to compute the field penetration using the same procedure as for the slab, provided that minor modifications in the computed quantities are made. Here we will give the modifications needed. Firstly, the normalization procedure is the same, with the same normalization factors. In this case the space variable x stands for the radius in the cylinder. The equations governing the penetration are:

$$\frac{\partial h}{\partial x} = \pm j \quad (2.16)$$

$$\frac{1}{x}\frac{\partial (xe)}{\partial x} = -\frac{\partial h}{\partial t} \quad (2.17)$$

where Eq. (2.16) is in fact identical to Eq. (2.1), while Eq. (2.17) contains terms that are originated from the *rot* differential operator in cylindrical symmetry. Because of the coincidence of Eqs. (2.1) and (2.16), the field penetration has the same solution, namely Eqs. (2.3) and (2.4). The electric field, on the other hand, is given by:

$$e = -\frac{\dot{h}_e}{2}\frac{x^2 - x_p^2}{x} \quad (2.18)$$

so that now the local dissipated power density is given by:

$$p = \frac{j\dot{h}_e}{2}\frac{x^2 - x_p^2}{x} \quad (2.19).$$

From Eq. (2.19) we compute the average power density in the cylinder:

$$\begin{aligned}\overline{p} &= \frac{1}{\pi}\int_{x_p}^{1}\frac{j\dot{h}_e}{2}\frac{x^2-x_p^2}{x}2\pi x dx \\ &= \frac{\dot{h}_e j}{3}\left(1-3x_p^2+2x_p^3\right)\end{aligned} \qquad (2.20).$$

The average volume magnetization is given in this case by:

$$\overline{m} = \frac{1}{\pi}\int_{0}^{1} h 2\pi x dx - h_e \qquad (2.21)$$

where the integral of a single shielding layer extending from $x_p^{\ n}$ to $x_p^{\ n+1}$ equals:

$$\begin{aligned}&\frac{1}{\pi}\int_{x_p^n}^{x_p^{n+1}} h 2\pi x dx = \\ &= 2h\left(x_p^n\right)\left(x_p^{n+1\,2}-x_p^{n\,2}\right)+\frac{2}{3}\frac{h\left(x_p^n\right)-h\left(x_p^{n+1}\right)}{\left(x_p^{n+1}-x_p^n\right)}\left(x_p^{n+1\,3}-x_p^{n\,3}\right)-x_p^n\frac{h\left(x_p^n\right)-h\left(x_p^{n+1}\right)}{\left(x_p^{n+1}-x_p^n\right)}\left(x_p^{n+1\,2}-x_p^{n\,2}\right)\end{aligned} \qquad (2.22)$$

3. Coupling loss

For the calculation of the coupling loss we make the assumption that the cable can be described macroscopically by three time constants τ_k and three demagnetization shape factors n_k[2]. Each time constant and demagnetization factor τ_k and n_k refer to a direction k in the cable. The convention is further that the first two directions are normal to the cable, while the third is parallel to the transport current. We have chosen this uniform treatment, that neglects a separate representation of parallel field losses, because there is a clear lack of evidence from experimental data that parallel field loss in a cable has a significant impact. The second assumption is that the cable is not saturated, and coupling currents can flow unperturbed in the cable. This hypothesis holds for operation far from the critical surface and sufficiently small field changes. As for hysteresis magnetization and loss, we will consider the three cable directions as completely independent, and solve for each direction independently from the other. Therefore we will drop the subscript k for the time constants and the demagnetization shape factors.

The first step in the calculation of the coupling current magnetization and loss is the integration of the equation for the internal field in the cable [1]:

$$\dot{B}_i + \frac{B_i}{\tau} = \frac{B_e}{\tau} \tag{3.1}$$

where B_i is the field in the composite and B_e is the external, changing field. If the external field is assumed to change linearly with time, i.e.:

$$B_e = B_e^0 + B_e^1 t \tag{3.2}$$

Eq. (3.1) can be solved, leading to the general integral:

$$B_i = B_e^0 + B_e^1 (t - \tau_k) + Ce^{-\frac{t}{\tau}} \tag{3.3}$$

where C is an arbitrary constant. The last term in Eq. (3.3) is a decaying exponential with time constant τ_k that describes the shielding phase for fast field changes. Once the exponential has decayed, the internal field is equal to the external field delayed by τ_k, as it is clear from the first two terms. Equation (3.3) must be specialized to match the initial condition on the internal field:

$$B_i(0) = B_i^0 \tag{3.4}$$

leading to the following complete solution for the internal field:

$$B_i = B_e^0 + B_e^1 (t - \tau) + \left[B_i^0 - \left(B_e^0 - B_e^1 \tau_k\right)\right] e^{-\frac{t}{\tau}} \tag{3.5}$$

and for the internal field derivative:

$$\dot{B}_i = B_e^1 - \frac{\left[B_i^0 - \left(B_e^0 - B_e^1 \tau\right)\right]}{\tau} e^{-\frac{t}{\tau}} \tag{3.6}.$$

From Eq. (3.6) we calculate the instantaneous magnetization and power dissipated as:

$$M = -\frac{n\tau}{\mu_0} \dot{B}_i \tag{3.7}$$

$$P = \frac{n\tau}{\mu_0} \dot{B}_i^2 \tag{3.8}$$

and finally the energy during a field swing:

$$E = \int_0^T P dt$$
$$= \frac{n\tau}{\mu_0} B_e^{1\,2} T - \frac{n}{2\mu_0}\left[B_i^0 - \left(B_e^0 - B_e^1\tau\right)\right]^2\left(e^{-2\frac{T}{\tau}} - 1\right) + \frac{2n\tau}{\mu_0} B_e^1\left[B_i^0 - \left(B_e^0 - B_e^1\tau\right)\right]\left(e^{-\frac{T}{\tau}} - 1\right) \quad (3.9).$$

For each field direction *k*, the calculation algorithm uses Eq. (3.5) to keep track of the internal field during a swing, and Eqs. (3.7), (3.8) and (3.9) to compute magnetization, instantaneous power and energy dissipated in the swing. The calculation must therefore keep track of the internal field at the end of the swing, that is used as initial condition for the following swing.

4. Examples

4.1 Hysteresis loss in a strand

The first test is a calculation of the hysteresis loss in a multifilamentary strand with cylindrical filaments submitted to a changing parallel or transverse field. We have taken a constant J_c value of 10^{10} A/mm^2 and a filament diameter of 100 μm. This case, of rather academic nature, has been chosen in order to compare the numerical results to known analytic solutions. We have computed the loss per cycle, taking a periodic variation of the external applied field, with a peak-to-peak amplitude B_m. The analytical solution for transverse field variation has been already given in Eq. (2.11). For parallel field variations the loss per cycle is given by:

$$Q = \begin{cases} \frac{B_m^2}{2\mu_0}\frac{2}{3}\left(\beta - \frac{\beta^2}{2}\right) & for\ \beta \le 1 \\ \frac{B_m^2}{2\mu_0}\frac{2}{3}\left(\frac{1}{\beta} - \frac{1}{3\beta^2}\right) & for\ \beta > 1 \end{cases} \quad (4.1)$$

where the parameter β is defined as given in Eq. (2.12), and, as discussed previously, the penetration field is identical to that of a slab of the thickness equal to the cylinder diameter, see Eq. (2.13). These analytical results are compared in Fig. 2 with the results of the calculation algorithm the we have proposed. Note that there we have normalised the results to the quantity $B_m^{\,2}/2\mu_0$ proportional to the magnetic energy variation.

As we expect, the results of the cylinder in parallel field are identical to those obtained analytically, the only difference between the calculations being the numerical integration of the energy from the average power dissipation in the filament instead of the analytical integration for this simple cycle. In the case of

the cylinder in transverse field, the scaled slab solution approximates very well the analytical result (which, in itself, is again only an approximation). The maximum error is around penetration, and is of the order of 20 %. We believe that this is an acceptable error, because of the high flexibility gained with our algorithm, that can treat any field cycle and delivers instantaneous power rather than energy dissipated in a closed field cycle.

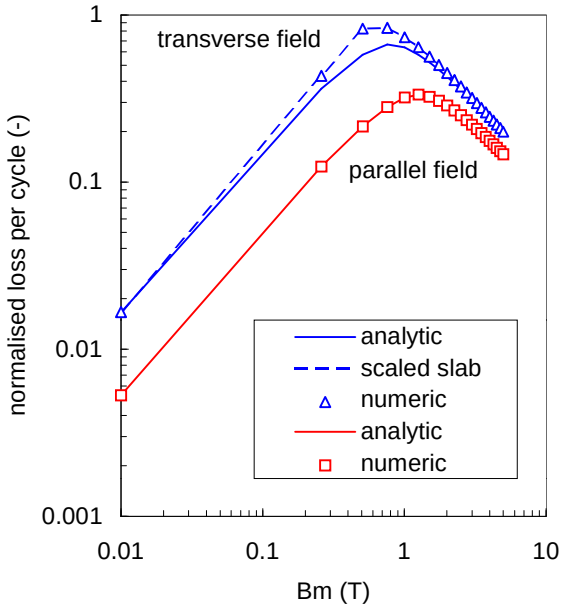

Figure 2. Comparison of analytical results and our algorithm for the calculation of the hysteresis loss per cycle in a cylindrical superconducting filament in parallel or transverse field, as a function of the peak-to-peak field swing B_m. The loss per cycle has been normalised to the magnetic energy change $B_m^2/2\mu_0$.

4.2 Coupling loss in a strand

As a second test, we have used the coupling loss algorithm to compute the coupling current loss in a strand with a time constant τ of 100 ms, subjected either to a single trapezoidal field cycle or to a continuous harmonic field variation. In both cases the amplitude of the field change was B_m. In the case of the trapezoidal field cycle we have taken equal ramp-up and ramp-down time T_m, and very long flat-top times (compared to the ramp time T_m). In the case of the harmonic field variation we have taken a period T, corresponding to an angular frequency $\omega = 2\pi/T$ The analytical solution for the case of a trapezoidal field cycle can be once more written in terms of the energy dissipated per cycle, and is given by:

$$Q = \frac{B_m^2}{2\mu_0}\frac{8\tau}{T_m}\left[1-\frac{\tau}{T_m}\left(1-e^{-\frac{T_m}{\tau}}\right)\right] \qquad (4.2).$$

Similarly for the continuous, harmonic field changes we can write:

$$Q = \frac{B_m^2}{2\mu_0}\frac{\pi\omega\tau}{\omega^2\tau^2+1} \qquad (4.3).$$

The comparison of the analytical and numerical solution in these two simple, but complete, cases is reported in Figs. 3 and 4. For the trapezoidal field variations the field changes linearly, and therefore only 4 field swings were necessary for the numerical solution (ramp-up, flat-top, ramp-down, flat-top). In the case of the harmonic variation, the periodic dependence of the field had to be approximated with piecewise linear segments. Care was taken for this approximation (typically 100 points were used to describe a complete waveform). In both cases the numerical solution obtained cannot be distinguished from the analytical one.

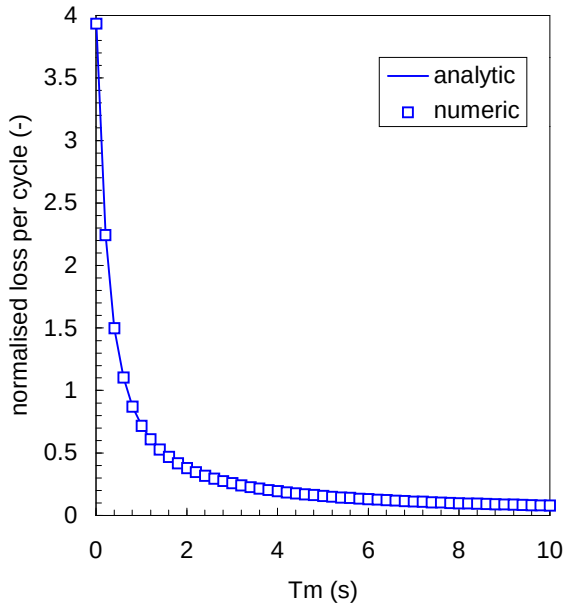

Figure 3. Comparison of analytical results and our algorithm for the calculation of the coupling loss per cycle in a strand subjected to a trapezoidal field cycle, as a function of the ramp time T_m. The loss per cycle has been normalised to the magnetic energy change $B_m^2/2\mu_0$.

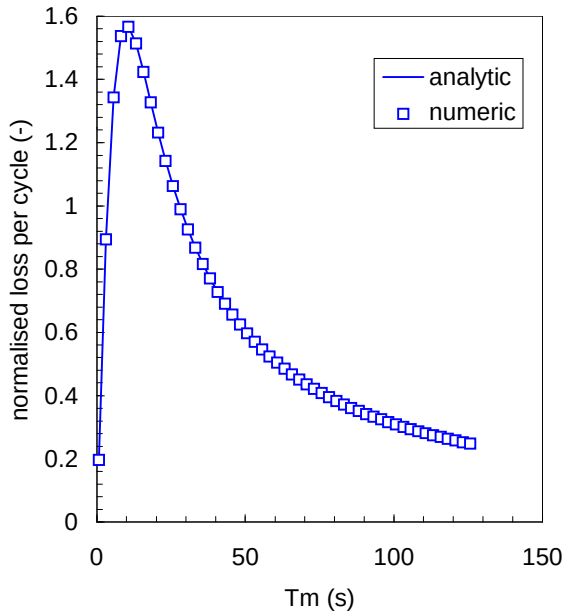

Figure 4. Comparison of analytical results and our algorithm for the calculation of the coupling loss per cycle in a strand subjected to a continuous, harmonic field variation, as a function of the period of the harmonic wave T. The loss per cycle has been normalised to the magnetic energy change $B_m^2/2\mu_0$.

References

[1] M. Wilson, *Superconducting Magnets*, Clarendon Press Oxford, 1983.

[2] A.M. Campbell, *A General Treatment of Losses in Multifilamentary Superconductors*, Cryogenics, **22**, 3, 1982